Indian Journal of Chemistry
Vol. 63, January 2024, pp. 15-20
DOI: 10.56042/ijc.v63i1.304

Peepal (*Ficus religiosa*) leaf extract mediated green synthesis of lanthanum and cerium oxide nanoparticles: Characterization and potential biological applications

Pranali Parab, Aniket Pawanoji* & Amol Pawar

Department of Chemistry, K. J. Somaiya College of Science and Commerce, Vidyavihar (E), Mumbai 400 077, India
E-mail: aniket@somaiya.edu

Received 3 April 2023; accepted (revised) 22 December 2023

The present study describes the synthesis of lanthanum and cerium oxide (La_2O_3 and CeO_2) nanoparticles (NPs) based on eco-friendly approach using *Ficus religiosa* leaves extract. The synthesized NPs have been characterized using various analytical techniques, including UV-Visible and FT-IR spectroscopy, and PXRD. The surface morphology and shape of the NPs have been determined using advanced imaging techniques such as Scanning Electron Microscope (SEM), Transmission Electron Microscope (TEM) and High-Resolution Transmission Electron Microscope (HRTEM) revealing that the NPs possessed predominantly spherical and rod-like shapes. Additionally, the surface area covered by NPs has been calculated using BET analysis and it shows an increment from a value of 7.243 $m^2\ g^{-1}$ to 45.144 $m^2\ g^{-1}$ and peak pore volume increases from 0.0743 $cm^3\ g^{-1}$ to 0.1904 $cm^3\ g^{-1}$. The antibacterial activity of NPs has been evaluated against Gram-positive and Gram-negative bacteria showing significant activity. Finally, the hemolytic and antioxidant activity of NPs have been assessed and have demonstrated their efficacy suggesting their potential applications.

Keywords: Lanthanum oxide nanoparticles, Cerium oxide nanoparticles, Transmission electron microscopy, Antioxidant, Green synthesis, Hemolysis

Nanotechnology is an emerging and rapidly growing technology. It has found to have remarkable applications for environmental science, medicine, drug delivery, and ceramic coating of walls[1]. The metal oxide nanoparticles bear potential applications plethora of numerous fields such as radiotherapy enhancement[2], diagnostic assay[3], thermal ablation[4], *etc*.

The metal oxide nanoparticles have been synthesized by various methods such as chemical synthesis[5], hydrothermal[6], solvothermal[7] and sol-gel method[8]. However, green synthesis has gained attention over other methods for preparing nanomaterials. Green synthesis is a simple, one-step, cost-effective, and eco-friendly method[9]. This method uses many bioactive agents such as microorganisms[10], fruit peels[11] and plant materials[12] as reducing agents[13]. It is reproducible, consumes less time and its by-products are non-hazardous to nature[14]. Many researchers already reported nanoparticles of transition metal oxides, but very few papers have been reported using inner-transition metals *via* the green route. Lanthanum and cerium oxide nanoparticles have a medicinal advantage due to their unique properties by making them cytotoxic for cancer-like treatments[15]. Therefore, there is a need to study the unique properties of nanoparticles of inner-transition metal oxides.

While following the green route, we primarily focus on two principles of green chemistry *i.e*., 'Less hazardous chemical synthesis' and 'Renewable feedstocks'. The green method is designed in such a manner that the plant acts as a natural reducing and capping agent[16], thereby, preventing the unnecessary addition of reagents and less consumption of hazardous chemicals to get desired compounds.

This paper presents the green synthesis of lanthanum oxide and cerium oxide nanoparticles using Peepal (*Ficus religiosa*) leaves extract. Traditionally, peepal leaves are used to treat heart diseases, jaundice, diabetes, bleeding, and to prevent itchiness of the skin[17]. The synthesized La_2O_3 and CeO_2 nanoparticles were characterized for their appearance, structural, and morphological properties and tested for the biological and hemolytic study.

Experimental Section

The chemicals used in the experiment had been procured from Loba Chemie and Alpha chemical laboratories. The *Ficus religiosa* (Peepal) leaves were plucked from the campus of the Somaiya Vidyavihar University (SVU), Mumbai, Maharashtra, India. The leaves were washed thoroughly to remove dust particles and air-dried.Approximately, 50 g leaves were

finely chopped, immersed in 250 mL of distilled water at 80-90 °C for 15 minutes, and filtered using Whatman filter paper no 41. 0.1 M Lanthanum solution, was prepared by dissolving 4.33g $La(NO_3)_3.6H_2O$ in distilled water. Lanthanum solution was mixed with leaf extract in the proportion of 1:5 and stirred for about 2 hrs at 80 °C to form a precipitate. The compound was collected using a centrifuge and washed with ethanol to remove any impurities and then the dried compound was pyrolyzed in a muffle furnace at 600 °C for 2 h to get La_2O_3. The final product was well-grounded using mortar and pestle for uniform particles. 0.1 M solution of cerium was prepared by weighing (4.34 g) of cerium nitrate $Ce(NO_3)_3.6H_2O$ salt dissolved in distilled water and the reaction protocol for La_2O_3 was followed. The schematic representation of the reaction is shown in Fig. 1.

Results and Discussion

The hydroxides of lanthanum and cerium are found to be greenish-brown in colour. These hydroxides were pyrolyzed to corresponding oxides at 600 °C. The obtained solids of lanthanum and cerium oxide nanoparticles were free-flowing, white and pale yellow in colour respectively.

UV-Visible Studies

UV-Visible spectra of synthesized nanoparticles have been conducted by UV- Lab India spectrophotometer. The UV-Visible spectrum of La_2O_3 and CeO_2 shows an intense peak at 200 nm and at 315 nm respectively which could be due to the intra-ligand π-π^* transition, confirming the formation of nanoparticles. The band gap was calculated using a Tauc's plot for nanoparticles and it was found to be 5.09 eV and 4.97 eV for La_2O_3 and CeO_2 respectively[18,19]. The bandgap in La_2O_3 is comparatively higher than other rare earth metals.

FTIR Studies

FTIR spectra were carried out for the nanoparticles in the range of 4000-400 cm^{-1}. Fig. 2a shows the FTIR spectra of La_2O_3 and CeO_2 nanoparticles. The broad bands appeared at 3431 cm^{-1} and 3401 cm^{-1} due to O-H stretching for La_2O_3 and CeO_2 respectively. The bands appear at 1463 cm^{-1} and 1384 cm^{-1} showing symmetric stretching of N-O. Furthermore, bands at 1084 cm^{-1} and 1022 cm^{-1} exhibit due to the wagging of C-H bonds. The band appeared at 514 cm^{-1} corresponding to (La-O) stretching[20]. The band at 1637 cm^{-1} and 1537 cm^{-1} are due to C=O stretching. Other bands at 1118 cm^{-1} and 998 cm^{-1} show the presence of Ce-O-Ce vibrations. The band appeared at 491 cm^{-1} corresponding to (Ce-O) stretching[21].

X-ray diffraction analysis

The purity and structural phase of La_2O_3 and CeO_2 has been determined by the X-ray Diffractometer. In the XRD pattern, peaks observed at 2θ angle correspond to crystallographic planes of 29.08° (222), 30.70° (400), 40.55° (134), 44.02°(440), 50.67° (541), 53.61° (622) for La_2O_3 NPs and for CeO_2 NPs are 28.95° (111), 33.30°(200), 47.78° (220), 56.72°(311), 59.12° (222), 69.96° (400) respectively. The XRD pattern (Fig. 2b) is well fitted for La_2O_3 (JCPDS no. –65-3185) which shows BCC structure and for CeO_2 (JCPDS no. –43-1002) with the Face centered cubic structure respectively. The crystallite size was measured using the Debye-Scherrer formula, $D = k\lambda/\beta\cos\theta$. The average crystallite size for La_2O_3 and CeO_2 is19.8 nm and 3.34 nm respectively.

SEM-EDS, HRTEM and SAED Analysis

SEM analysis is a useful tool to study the morphology of synthesized nanomaterials. The SEM images of La_2O_3 and CeO_2 NPs were recorded using Zeiss, Ultra plus, Oxford company INCA with an energy source of 15 kV. The surface of synthesized nanoparticles is smooth and shows irregular rod and spherical shapes morphology with various magnifications. The clustered particles found are due to the excess quantity of leaf extract.

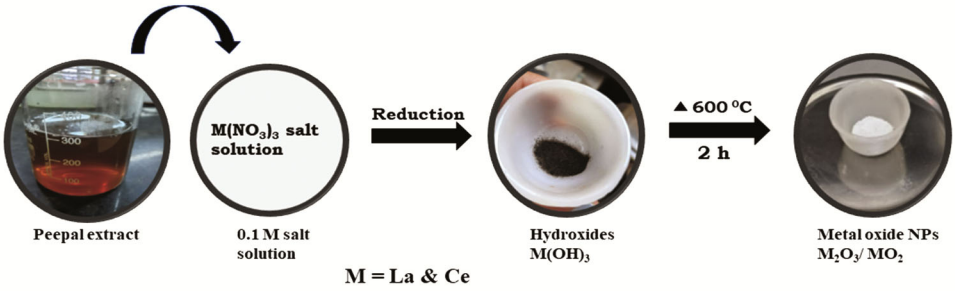

Fig. 1 — Experimental procedure for the preparation of La_2O_3 and CeO_2 nanoparticles using *Ficus religiosa* leaves extract

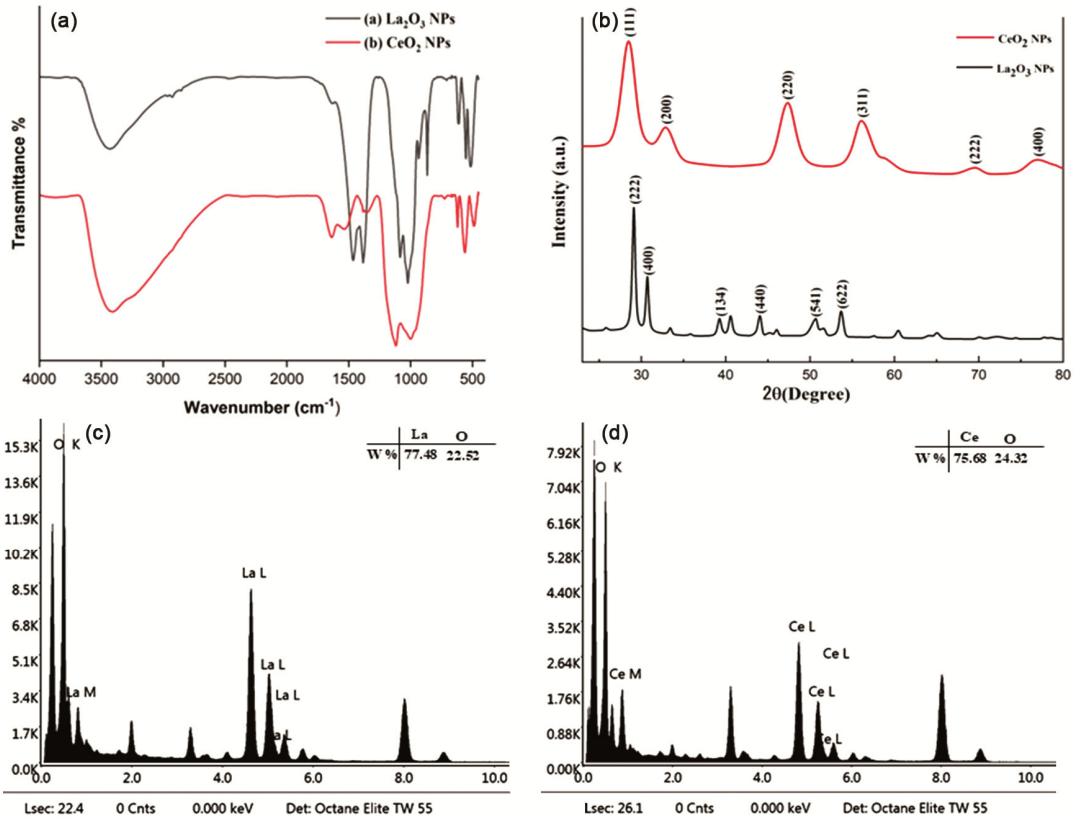

Fig. 2 — (a) FTIR (b) XRD pattern of La_2O_3 and CeO_2, EDS images of (c) La_2O_3, (d) CeO_2

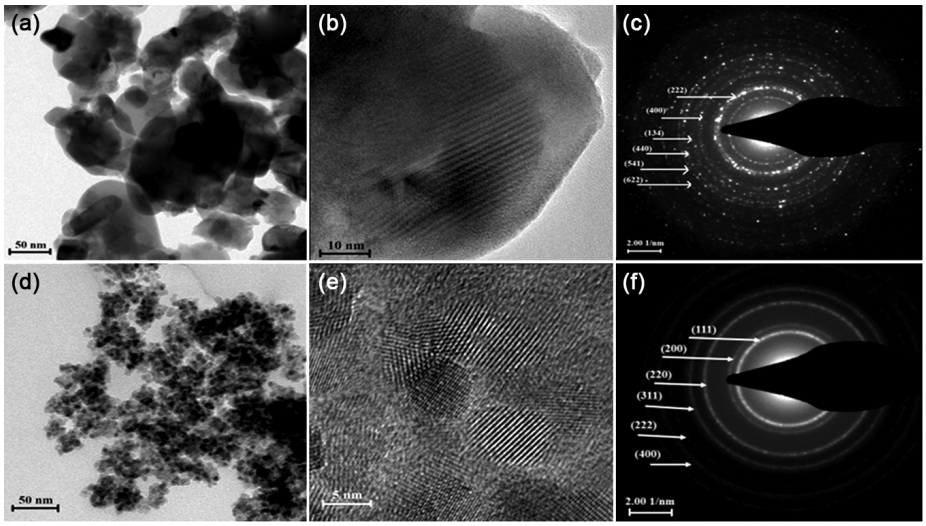

Fig. 3 — TEM images of (a) La_2O_3 and (d) CeO_2, HRTEM images (b) La_2O_3 and (e) CeO_2, SAED pattern of (c) La_2O_3 and (f) CeO_2 nanoparticles

In EDS (Fig. 2c and Fig. 2d) spectra of La_2O_3, the percentage of lanthanum and oxygen are 77.48 and 22.52 respectively in weight percentage whereas in the case of CeO_2, Cerium is 75.68% and oxygen is about 24.32% which confirms the purity of the prepared nanoparticles.

HRTEM analysis (Fig. 3) was carried out using FEI, Tecnai G2, F30 TEM, an accelerating voltage of 300 kV, Megaview III camera, and Soft Imaging Systems iTEM software. The obtained nanoparticle size ranges between 5-50 nm, which agrees with the average size calculated from the Debye-Scherrer

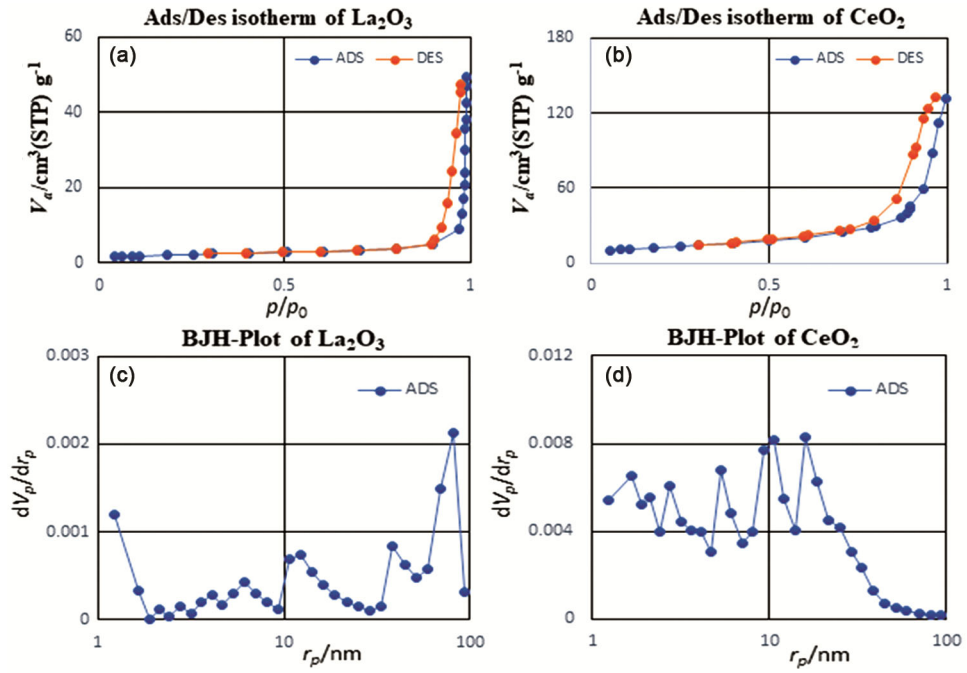

Fig. 4 — Ads-Des. of (a) La_2O_3 and (b) CeO_2, BJH plot of (c) La_2O_3 and (d) CeO_2

Table 1 — Surface area analysis of synthesized La_2O_3 and CeO_2 NPs.

S. No.	Sample Name	BET surface area ($m^2\ g^{-1}$)	Peak Pore Volume ($cm^3\ g^{-1}$)	Peak pore Sizes (nm)
1	La_2O_3	07.243	0.0742	81.60
2	CeO_2	45.144	0.1904	16.14

formula. The planes of SAED patterns Fig. 3c and Fig. 3f were calculated and matched with XRD data. The spacing of crystallographic planes from the SAED pattern for La_2O_3 is 0.30 nm, 0.29 nm, 0.22 nm, 0.20 nm, 0.17 nm and 0.16 nm corresponding to the characteristic planes at (222), (400), (134), (440), (541) and (622). For CeO_2, the spacing of crystallographic planes is 0.33 nm, 0.29 nm, 0.21 nm, 0.17 nm, 0.14 nm and 0.13 nm which correspond to the (111), (200), (220), (311), (222) and (400). The dotted rings (Fig. 3c) in the SAED pattern further indicate highly crystalline nature of La_2O_3 nanoparticles and in (Fig. 3f) slightly crystalline nature of CeO_2.

BET analysis

The surface area and pore size distribution of synthesized nanoparticles were estimated using the BET (Fig. 4a and Fig. 4b) method. The data obtained from surface area analysis is presented in Table 1. The isotherms indicate adsorption hysteresis behaviour in the P/P° ~ 0.4 to 0.99, with a mixture of mesoporous and macroporous structures. The surface area shows an increment value from 7.243 $m^2\ g^{-1}$ to 45.144 $m^2\ g^{-1}$ and peak pore volume from 0.0743 $cm^3\ g^{-1}$ to 0.1904 $cm^3 g^{-1}$. This increment in surface area and peak pore volume is attributed to the decrement in particle sizes and subsequent peak pore sizes of as-synthesized materials. The peak pore size of La_2O_3 and CeO_2 is 81.60 and 16.14 nm respectively. The pore distribution plot of synthesized NPs was determined by BJH (Barrett-Joyner-Halenda) method shown in Fig. 4c and Fig. 4d. A multimodal peak in the plotted graph is due to the non-uniform size of NPs and their mesoporous nature.

Antibacterial activity

The antibacterial activity of synthesized La_2O_3 and CeO_2 nanoparticles was studied using the Disc diffusion method. This activity was studied against Gram-positive bacteria such as S. aureus and B. subtilis and Gram-negative bacteria such as K. pnuemoniae and Shigella. The molten nutrient agar medium was uniformly spread on the glass plate to form a solid layer. Further, overnight-grown bacterial

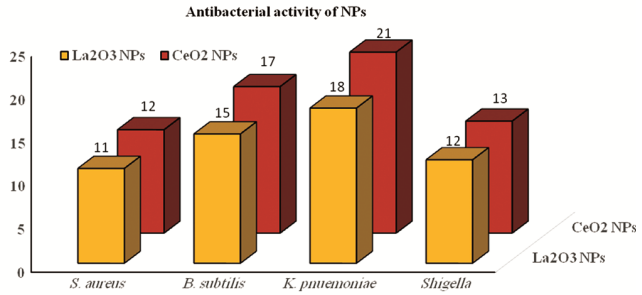

Fig. 5 — Antibacterial studies of S. aureus, B. subtilis, K. pnuemoniae & Shigella against La_2O_3 and CeO_2 NPs

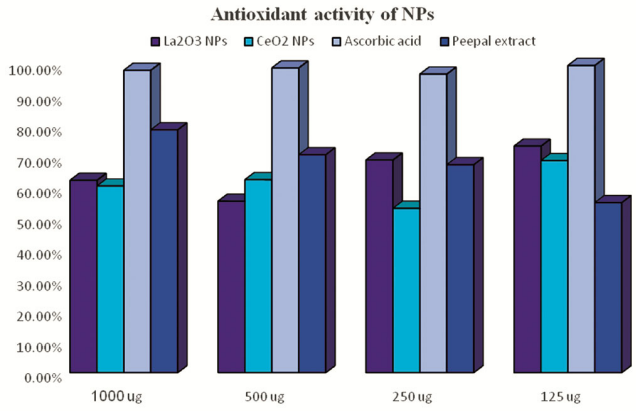

Fig. 6 — Antioxidant activity of synthesized nanoparticles

cultures were introduced. The 6mm disks dipped in the solution of synthesized nanoparticles were placed on cultured media. All the cultured plates were kept in an incubator at 37 °C. The inhibition zone was observed for the period of 24-48 hours after incubation and measured using a scale; the values are given in the following 3-D column chart (Fig. 5).

Hemolysis study

The very purpose of performing a hemolysis assay is to determine the ability of the nanomaterials to destroy RBCs which leads to the release of haemoglobin. In the hemolysis study, human red blood cells were tested against nanomaterials and are co-incubated in a buffer solution at definite *p*H. In this procedure, the blood of a healthy human was collected in tubes containing the anti-coagulant chemical 0.1 M EDTA. The nanomaterials used in this test were prepared in Phosphate buffer saline (PBS) solution at 7.4 *p*H. These prepared samples were placed in a sterilized medium and incubated under static conditions at RT for 3 hrs. PBS was used as the negative control and distilled water as a positive control. The samples containing tubes were then centrifuged and absorbance of the supernatant was measured at 541 nm. The hemolysis ratio (Z) was calculated using the following formula, $Z = (D_t - D_{nc}) / (D_{pc} - D_{nc}) * 100$.

Where Z = hemolysis ratio

D_t = test samples

D_{nc} = negative controls

D_{pc} = positive controls

The experiment was performed in triplicate and the obtained values for the La_2O_3 and CeO_2 nanoparticles in this experiment are around 3.01% and 2.78% respectively, indicating a slightly hemolytic nature[22].

Antioxidant activity of NPs

A substance's antioxidant nature inhibits nutrient oxidation by preventing oxidative chain reactions as it is synthesized using peepal leaf extract. Peepal leaves due to the presence of different functional groups are used to measure the inhibition rate termed as antioxidant activity. Free radical scavenging (Antioxidant activity) of synthesized NPs was widely determined by DPPH assay. The purpose of using DPPH is that it is simple, rapid and stable. Ascorbic acid was used as a standard. 0.2 mM methanolic solution of DPPH was prepared and used as positive control. Different concentrations of synthesized NPs were prepared in methanol and a 1:1 ratio was maintained between methanol and DPPH. The reaction mixture was incubated for half an hour at RT and absorbance was measured at 517 nm indicating absorbance gradually decrease with time. The increase in antioxidant activity of NPs is directly proportional to the disappearance of the purple colour. This decolouration indicates the scavenging activity of nanoparticles. The obtained results were compared with standard values of ascorbic acid and peepal extract[23] which shows the moderate antioxidant activity of synthesized La_2O_3 & CeO_2NPs. The results revealed that the NPs are free radical inhibitors that can possibly act as primary antioxidants due to functional groups bound to them[24,25].

This experiment was performed in duplicate and the obtained results are given in Fig. 6, as the concentration was decreased, the percentage of peepal leaves extract also decreased and % of NPs increased. The % of Radical scavenging activity was calculated by using the following formula, % Radical Scavenging activity = [(Absorbance control − Absorbance sample) / Absorbance control] × 100.

Conclusion

La_2O_3 and CeO_2 nanoparticles were successfully synthesized using an aqueous extract of *Ficus religiosa* leaves. UV-Visible, FTIR, and PXRD analysis confirmed the optical behaviour, vibrational modes, and size of synthesized La_2O_3 and CeO_2 NPs. The surface morphology and shape were determined by performing the SEM, TEM and HR-TEM techniques reveal that NPs are spherical or rod-like in shape with an average crystallite size of 5-50 nm. BET analysis was carried out to measure the surface area covered by solid nanoparticles. The antibacterial activity of synthesized nanoparticles was performed against overnight grown bacteria to view its inhibited growth zone. Hemolytic studies were carried out to check the toxicity of NPs on RBCs and results show that the samples are slightly hemolytic. The antioxidant activity of synthesized NPs exhibits good results and may have potential applications in the field of biomedicine and material science. Overall, this study highlights the potential of using *Ficus religiosa* leaves extract as a green and sustainable method for synthesizing La_2O_3 and CeO_2 nanoparticles with promising properties such as high surface area, good antibacterial and antioxidant activity with the low hemolytic assay.

Acknowledgement

It is a self-funded project. The authors want to extend their sincere gratitude to the Department of Chemistry, Microbiology and Botany from K. J. Somaiya College of Science and Commerce, Vidyavihar for providing the necessary facilities. We further thank SAIF-IIT Bombay, Tata Institute of Fundamental Research (TIFR) and Dr. Rohant Dhabbe, Jaysingpur College Jaysingpur, Maharashtra, India for providing characterization facilities.

References

1 Nazaripour E, Mousazadeh F, Moghadam M D, Najafi K, Borhani F, Sarani M, Ghasemi M, Rahdar A, Iravani H S & Khatami M, *Inorg Chem Commun*, 131 (2021) 108800.
2 Hainfeld J F, Dilmanian F A, Slatkin D N & Smilowitz H M, *J Pharm Pharmacol*, 60 (2008) 977.
3 Pandiyan N, Murugesan B, Arumugam M, Chinnalagu D K, Selvaraj R, Azhagar S & Mahalingam S, *Photochem Photobiol*, 202 (2019) 111706.
4 KannanS K & Sundrarajan M, *J Nanosci*, 13 (2014) 1450018.
5 De Souza C D, Nogueira B R, Elisa M & Rostelato C M, *J Alloys Comp*, 798 (2019) 714.
6 Meng L, Wang B, Ma M & Lin K, *Mater Today Chem*, 1 (2016) 63.
7 Han S, Kong M, Guo Y & Wang M, *Mater Lett*, 63 (2009) 1192.
8 Majid D, Javad H S, Reza K O, Ali H H, Leila G & Sina G, *Ceram Int*, 40 (2014) 7425.
9 Velsankar K, Suganya S, Muthumari P, Mohandoss S & Sudhahar S, *J Environ Chem Eng*, 9 (2021) 106299.
10 Zhang X, Yan S, Tyagi R D & Surampalli R Y, *Chemosphere*, 82 (2011) 489.
11 Yulizar Y, Juliyanto S, Sudirman, Apriandanu D O B & Surya R M, *J Mol Struct*, 1231 (2021) 129904.
12 Pandiyan N, Murugesan B, Sonamuthu J, SamayananS & Mahalingam S, *J Photochem Photobiol*, 178 (2018) 481.
13 Pandiyan N, Murugesan B, Sonamuthu J, Samayanan S & Mahalingam S, *Ceram Int*, 9 (2019) 12138.
14 Maheshwaran G, Muneeswari R S, Bharathi A N, Kumar M K & Sudhahar S, *Mater Lett*, 283 (2021) 128799.
15 Ayyakannu A, Chandrasekaran K, Abdulrahman S H H, Kasi G, Shanmugam G & Viswanathan K, *Mater Sci Eng*, 49 (2015) 408.
16 Amalina S N, Sukri M, Shameli K, Wong M M, Teow S, Chew J & Ismail N A, *J Mol Struct*, 1189 (2019) 57.
17 Janghel V, Patel P & Chandel S S, *Ann Hepatol*, 18 (2019) 658.
18 Naikoo G A, Mustaqeem M, Hassan I U, Awan T, Arshad F, Salim H & Qurashi A, *J Saudi Chem Soc*, 25 (2021) 101304.
19 Vanathi P, Rajiv P, Narendhran S, Rajeshwari S, Rahman P K & Venckatesh R, *Mater Lett*, 134 (2014) 13.
20 Ali M, Ikram M, Ijaz M, Ul-Hamid A, Avais M & Anjum A A, *Appl Nanosci*, 10 (2020) 3787.
21 Ezhilarasi A A, Vijaya J J, Kaviyarasu K, Kennedy L J, Jothiramalingam R & Al-Lohedan H A, *J Photochem Photobio*, 180 (2018) 39.
22 Padmanabhan V P, Narayanan S T S, Sagadevan S, Hoque M E & Kulandaivelu R, *Royal Soc Chem*, 43 (2019) 18484.
23 Koirala B, Pakuwal E, Rai H J & Shrestha A, *Int J Env*, 10 (2022) 48.
24 Mittal A K, Kaler A & Banerjee U C, *Nano Biomed Eng*, 4 (2012) 118.
25 Menon S, Devi K S S, Agarwal H & Shanmugam V K, *Colloid Interface Sci Comm*, 29 (2019) 1.